

An Ultra-low Voltage Blue Phase LCD for Mobile Applications

Jiamin Yuan, Daming Xu, and Shin-Tson Wu

College of Optics and Photonics, University of Central Florida, Orlando, Florida 32816

Abstract

We report an ultra-low voltage (<5V) two-domain blue phase liquid crystal display (BPLCD) for mobile applications. Compared to fringe field switching, our BPLCD shows superior performance in response time, integrated transmittance, viewing angle, and color shift. It also enables color sequential display with tripled optical efficiency and resolution density.

Author Keywords

Blue phase; liquid crystal display; mobile display.

1. Introduction

During the past decade, the rapid development of mobile displays, including touch-panel smart phones and tablets, revolutionarily changed our lives. In the meantime, the demand for better display performance is ever-increasing, such as low voltage and high transmittance for long battery life, wide viewing angle for multi-viewers, pressure-resistance for touch screen, etc. Fringe field switching (FFS) LCD [1], which shows superb performance in these aspects, is commonly implemented in mobile display devices. As a matter of fact, Apple's iPhone 6 uses two-domain FFS with a negative dielectric anisotropy liquid crystal (n-FFS) [2, 3]. However, the response time of n-FFS, which is typically ~20ms [4], is somewhat too slow for displaying fast-changing images as it causes image blurs. In the past, the feature of fast response time was mainly emphasized for LCD TVs as users preferred to watch movies on large-screen TVs. However, nowadays users tend to use their smartphones or tablets for movies and games more often. Therefore, there is an urgent need to develop fast-response LCDs for mobile displays while maintaining other high performances of n-FFS.

Polymer-stabilized blue phase liquid crystals (PS-BPLCs) [5, 6] are promising candidates for next-generation displays. PS-BPLCs exhibit several attractive features such as submillisecond response times [7-9], no need for surface alignment, and an optically isotropic dark state. After one decade of extensive efforts, major technical barriers of PS-BPLCs have gradually been overcome. Their operation voltage has been reduced from 50 V to below 10 V by employing large Kerr constant BPLC materials [10-12] and implementing device structures with enhanced penetrating fields [13-15]. High transmittance (>80%) can be achieved by optimizing the refraction effect of the non-uniform fringing electric fields [16].

In this paper, we report the device design and simulation results of a blue phase liquid crystal display (BPLCD) for mobile applications. By using a 3.5- μm protrusion electrodes and a large Kerr constant BPLC material, we are able to lower the operation voltage to <5V. Meanwhile, its submillisecond response time enables higher integrated transmittance than n-FFS. By using color-sequential display, both optical efficiency and resolution density can be further tripled. Moreover, BPLCD possesses better color performance and viewing angle than n-FFS. Therefore, BPLCD holds great potential for next-generation mobile display applications.

2. Low operation voltage

Protrusion and etching electrodes are two effective approaches to achieve low-voltage BPLCD by enhancing the penetration depth of electric field. Taking protrusion electrode as an example, the operation voltage of BPLCD is reduced dramatically as the protruded electrode height increases. By employing 2- μm protrusion electrode and using BPLC material JC-BP06 (JNC, Japan), the operation voltage could be reduced to <10V. Although this is an important milestone to enable a-Si TFT driving for BPLC, 10V is still too high for low-power mobile displays. However, it was reported that recently AU Optronics (Taiwan) has successfully fabricated protrusion electrodes with 3.5 μm height [17]. Hence, here we combine the 3.5 μm protrusion electrodes with a large Kerr constant material to reduce the operation voltage of BPLCD to ~5V for mobile display applications.

The BPLC material employed in our simulation is JC-BP07 [18] ($\Delta n_s=0.095$, $E_s=2.15\text{V}/\mu\text{m}$). To make a fair comparison between BPLCD and current n-FFS, we chose a negative LC with low viscosity and high dielectric anisotropy, named ZOC-7003 (JNC, Japan) [3], whose physical properties are as follows: $K_{11} = 13.0$ pN, $K_{22} = 7.0$ pN, $K_{33} = 16.7$ pN, $\Delta\epsilon = -4.36$, $\gamma_1 = 93.3$ mPas and $\Delta n = 0.103$ at $\lambda = 550$ nm. The cell gap of n-FFS is optimized at 550nm with $d\Delta n = 320\text{nm}$ whereas the cell gap of BPLC cell is 10 μm .

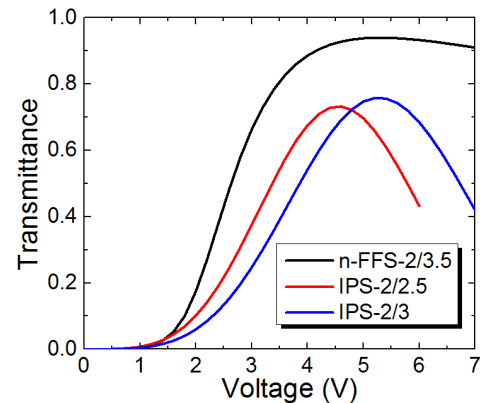


Figure 1. Simulated VT curves of nematic 1D n-FFS-2/3 and BPLC cells: IPS-2/2.5 and -2/3 ($\lambda = 550\text{nm}$).

Figure 1 compares the simulated voltage-transmittance (VT) curve of single-domain (1D) IPS 2/2.5 and -2/3 with 3.5- μm protrusion electrodes with that of 1D FFS-2/3, and the numerical values of their peak transmittance (T_{max}) along with operation voltage (V_{on}) are listed in Table I. It clearly shows that both IPS-2/2.5 and -2/3 are able to achieve lower operation voltage than n-FFS; in particular, the operation voltage of IPS-2/2.5 is reduced to 4.4V. However, both 1D IPS-BPLC and FFS suffer from color shift and grayscale inversion, which is the main reason that two-domain (2D) n-FFS is implemented in iPhone 6 and iPad Air 2. So to make our simulation results closer to the real products, we also compared the VT characteristics of 2D IPS-BPLC with those of 2D n-FFS. Their T_{max} as well as V_{on} are also listed in Table I. Here, the length of each arm for zigzag

electrodes is set at $20\mu\text{m}$. Due to dead zones at the turning corners of the zigzag electrodes, the T_{max} of 2D modes is reduced compared to that of corresponding 1D mode. Nevertheless, IPS-BPLC still shows lower V_{on} than n-FFS, which is very attractive for enabling longer battery life. Although the peak transmittance of IPS-BPLC cells is lower than that of n-FFS, their integrated transmittance turns out to be even higher than that of n-FFS due to the fast response time of BPLC, as will be outlined below.

Table 1. Simulated T_{max} and V_{on} of 1D and 2D n-FFS and IPS-BPLC cells ($\lambda = 550\text{ nm}$).

	T_{max}	V_{on}
1D FFS-2/3	94.0%	5.4V
1D IPS-2/2.5	73.3%	4.4V
1D IPS-2/3	75.8%	5.2V
2D FFS-2/3	87.2%	6.1V
2D IPS-2/2.5	67.6%	4.3V
2D IPS-2/3	70.3%	5.0V

3. High integrated transmittance

Despite IPS-BPLC has a lower peak transmittance than n-FFS (Fig. 1), its integrated transmittance, or luminance, perceived by human eyes is actually higher. Although high T_{max} has always been emphasized for LCDs, response time also plays an important role in enabling more light perceived by human eyes. Figure 2 depicts the time-transmittance (TT) curves of 2D IPS-BPLC and n-FFS cells in a single frame with a 60-Hz frame rate, same as iPhone 6. The response time of n-FFS is hardly reaching its peak transmittance in one frame, albeit the viscosity of ZOC-7003 is fairly low, leading to a reduced brightness. In contrast, the fast response time of IPS-BPLC earns itself more advantages. By integrating the transmittance over the whole frame (color areas in Fig. 2), which is the actual luminance perceived by human eyes, IPS-BPLC exhibits a higher average transmittance than n-FFS (68.0% vs. 59.6%), as shown by the color areas in Fig. 2. Also, due to fast decay time, BPLC shows reduced a crosstalk between two consecutive frames. More attractively, with its submillisecond response time, IPS-BPLC enables color-sequential display with negligible color breakup [19]. By eliminating the spatial color filters, the optical efficiency and resolution density are tripled, implying that our IPS-BPLC would be a very strong contender for power-saving and high-resolution mobile display applications.

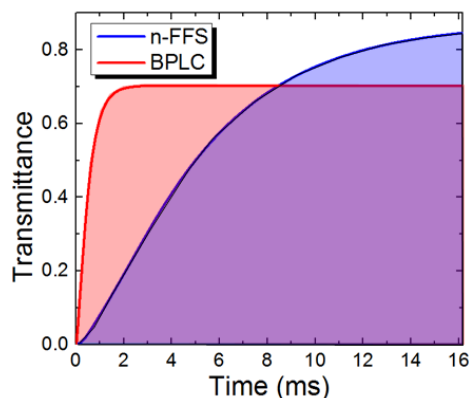


Figure 2. Simulated temporal transmittance curves of the 2D IPS-BPLC and n-FFS cells. (Frame rate: 60Hz)

4. Wide viewing angle

Moreover, IPS-BPLC also shows a much wider viewing angle than n-FFS. It is known that BPLC is optically isotropic in voltage-off state so that an excellent on-axis dark state can be obtained. However, polarizers are no longer crossed at oblique view and there is light leakage at dark state. For the wide-view purpose, a biaxial film is added before the analyzer to reduce the off-axis light leakage in the dark state. The parameters of biaxial film are as follows: $n_x = 1.521$, $n_y = 1.519$, and $n_z = 1.520$ and thickness of $137.5\mu\text{m}$. The n_x axis is parallel to the absorption axis of analyzer. The simulated isocontrast contour plots of film-compensated 2D IPS-BPLC and n-FFS are depicted in Figs. 3(a) and 3(b), respectively. It is shown that the viewing zone of IPS-BPLC with $>4000:1$ contrast ratio is over 30° , which is much better than that of n-FFS. Moreover, the viewing angle of IPS-BPLC is very symmetric and the viewing zone with $>100:1$ contrast ratio is over 85° , making IPS-BPLC an excellent candidate for high-end mobile displays.

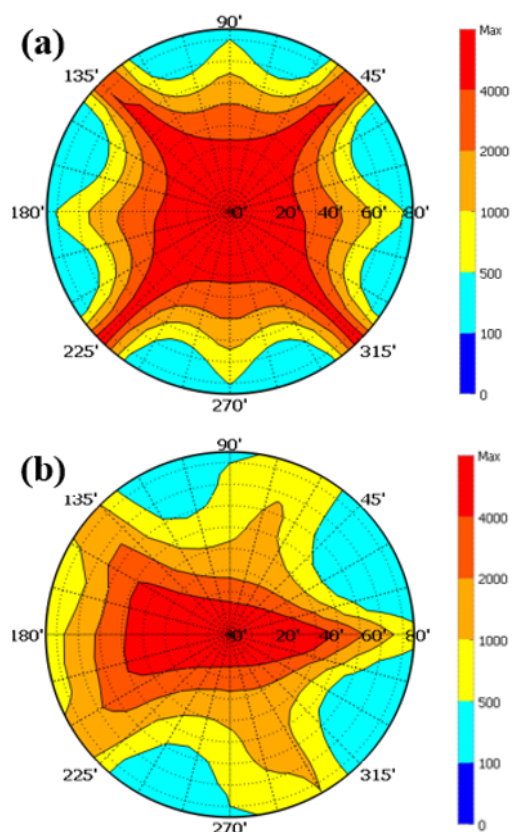


Figure 3. Isocontrast plots of biaxial-film-compensated (a) 2D IPS-2/3 and (b) 2D n-FFS.

To evaluate the off-axis image quality, the grayscale inversion is also simulated, as depicted in Figs. 4(a) and 3(b) are gamma curves of 2D IPS-BPLC and 2D n-FFS, respectively. The transmittance data is transformed into gamma curve based on the equation of $T = (GL/255)^{2.2}$, where GL stands for gray level. A negligible gray inversion occurs at G255 with 100.38% transmittance in IPS-BPLC, whereas n-FFS has a more severe gray inversion with 102.37% transmittance at G252. To better compare their gray inversions quantitatively, we use the off-axis image distortion index $D(\theta, \square)$ defined as [20]:

$$D(\theta, \phi) = \left\langle \frac{|\Delta T_{i,j(\text{on-axis})} - \Delta T_{i,j(\text{off-axis}, \theta, \phi)}|}{\Delta T_{i,j(\text{on-axis})}} \right\rangle_{i,j=0-255} \quad (1)$$

where $\Delta T_{i,j}$ stands for the transmittance difference between i^{th} and j^{th} gray levels, and $\langle \rangle$ denotes the average for all cases of arbitrary grays. The $D(\theta, \square)$ value ranges from 0 to 1. Our simulation results show that IPS-BPLC and n-FFS cells have D values of 0.107 and 0.205, respectively. The ~2X smaller off-axis gamma distortion of IPS BPLCD indicates it has better off-axis image quality, which is attributed to its self-compensation effect originating from the less uniform LC directors distribution since induced birefringence ellipsoid is along the direction of electric field. In contrast, the LCs in n-FFS rotate in horizontal plane more uniformly, leading to a larger gamma distortion at oblique view.

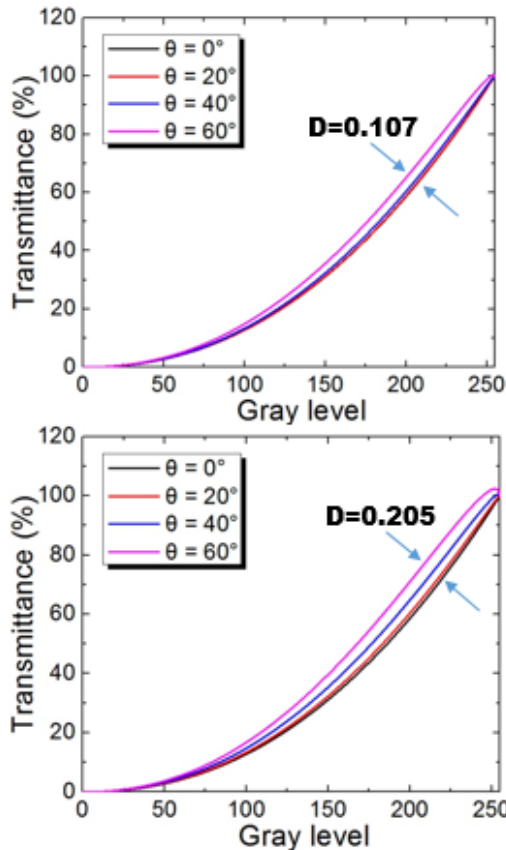


Figure 4. Viewing angle dependence of gamma curves for (a) 2D IPS-BPLC and (b) 2D n-FFS along the diagonal direction ($\square = 45^\circ$).

5. Unnoticeable color shift

Color shift is an important parameter describing the angular dependent color uniformity of a LCD system. Figure 5(a) depicts the color shift of film-compensated 2D IPS-BPLC using a white LED backlight in CIE 1976 diagram from different incident angles at the full-bright gray level G255 and the color difference is plotted in Fig. 5(b). The most severe color shift occurs at $\square = 45^\circ$, where the incident light experiences the largest birefringence. Hence, we fix \square at 45° and scan the incident angle θ across $-80^\circ \sim 80^\circ$ at 10° step. The IPS-BPLC cell exhibits a very small color shift: the most severe one is blue primary, with a color difference $\Delta u'v' = 0.0125$, which is below

the sensitivity of human eye ($\Delta u'v' = 0.02$). Therefore, the color shift of IPS-BPLC is unnoticeable by human eyes.

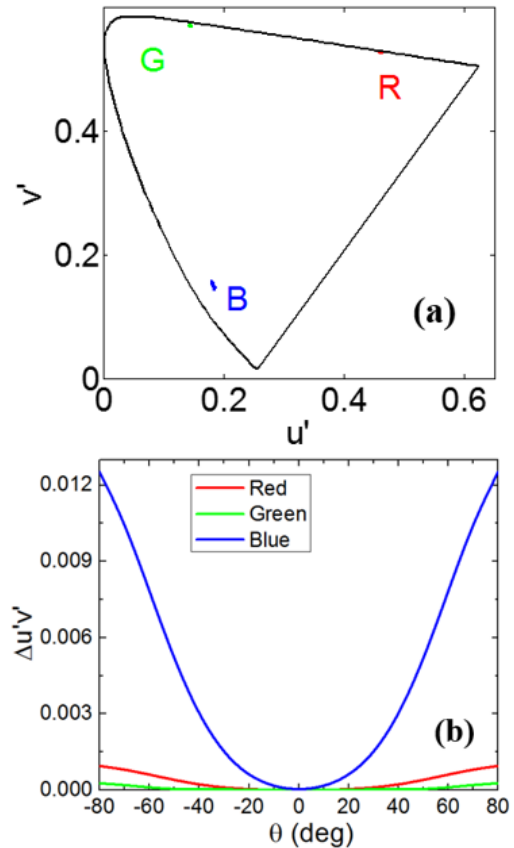


Figure 5. Color shift of RGB primaries in the film-compensated 2D IPS-BPLC at 45° azimuthal angle with incident angle varying from $-80^\circ \sim 80^\circ$: (a) positions in CIE 1976 and (b) color difference.

6. Impact

We proposed an IPS-BPLCD with an ultra-low operation voltage for mobile display applications. In addition, it also possesses other superior performance, such as fast response time, high transmittance, wide viewing angle, unnoticeable color shift and alignment-free fabrication. Hence, IPS BPLCD holds great potential for high-end mobile display applications.

7. References

- [1] S. H. Lee, S. L. Lee and H. Y. Kim, "Electro-optic characteristics and switching principle of a nematic liquid crystal cell controlled by fringe-field switching," *Appl. Phys. Lett.* **73**, 2881-2883 (1998).
- [2] Y. Chen, F. Peng, T. Yamaguchi, X. Song, and S. T. Wu. "High performance negative dielectric anisotropy liquid crystals for display applications," *Crystals* **3**, 483-503 (2013).
- [3] Y. Chen, Z. Luo, F. Peng, and S. T. Wu, "Fringe-field switching with a negative dielectric anisotropy liquid crystal," *J. Disp. Technol.* **9**, 74-77 (2013).
- [4] H. Chen, F. Peng, Z. Luo, D. Xu, S.T. Wu, M.C. Li, S.L. Lee, and W.C. Tsai, "High performance liquid crystal displays with a low dielectric constant material," *Opt. Mater. Express* **4**, 2262-2273 (2014).

- [5] H. Kikuchi, M. Yokota, Y. Hisakado, H. Yang, and T. Kajiyama, "Polymer-stabilized liquid crystal blue phases," *Nature Mater.* **1**, 64 (2002).
- [6] F. Peng, Y. Chen, J. Yuan, H. Chen, S.-T. Wu, and Y. Haseba, "Low temperature and high frequency effects on polymer-stabilized blue phase liquid crystals with large dielectric anisotropy," *J. Mater. Chem. C.* **2**, 3597-3601 (2014).
- [7] K. M. Chen, S. Gauza, H. Q. Xianyu, and S. T. Wu, "Submillisecond gray-level response time of a polymer-stabilized blue-phase liquid crystal," *J. Disp. Technol.* **6**, 49 (2010).
- [8] Y. Chen, J. Yan, J. Sun, S. T. Wu, X. Liang, S. H. Liu, P. J. Hsieh, K. L. Cheng, and J. W. Shiu, "A microsecond-response polymer-stabilized blue phase liquid crystal," *Appl. Phys. Lett.* **99**, 201105 (2011).
- [9] D. Xu, J. Yan, J. Yuan, F. Peng, Y. Chen, and S.T. Wu, "Electro-optic response of polymer-stabilized blue phase liquid crystals," *Appl. Phys. Lett.* **105**, 011119 (2014).
- [10] M. Wittek, N. Tanaka, D. Wilkes, M. Bremer, D. Pauluth, J. Canisius, A. Yeh, R. Yan, K. Skjonnemand, and M. Klasen-Memmer, "New Materials for Polymer-Stabilized Blue Phase," *SID Int. Symp. Dig. Tech. Pap.* **43**, 25-28 (2012).
- [11] Y. Chen, D. Xu, S. T. Wu, S. Yamamoto, and Y. Haseba, "A low voltage and submillisecond-response polymer-stabilized blue phase liquid crystal," *Appl. Phys. Lett.* **102**, 141116 (2013).
- [12] Y. Haseba, S. Yamamoto, K. Sago, A. Takata, and H. Tobata, "Low-Voltage Polymer-Stabilized Blue-Phase Liquid Crystals," *SID Int. Symp. Dig. Tech. Pap.* **44**, 254-257 (2013).
- [13] L. Rao, Z. Ge, S. T. Wu, and S. H. Lee, "Low voltage blue-phase liquid crystal displays," *Appl. Phys. Lett.* **95**, 231101 (2009).
- [14] L. Rao, H. C. Cheng, and S. T. Wu, "Low voltage blue-phase LCDs with double-penetrating fringe fields," *J. Disp. Technol.* **6**, 287-289 (2010).
- [15] H. Lee, H. J. Park, O. J. Kwon, S. J. Yun, J. H. Park, S. Hong, and S. T. Shin, "The world's first blue phase liquid crystal display," *SID Symp. Dig.* **42**, 121-124 (2011).
- [16] D. Xu, Y. Chen, Y. Liu, and S. T. Wu, "Refraction effect in an in-plane-switching blue phase liquid crystal cell," *Opt. Express* **21**, 24721-24735 (2013).
- [17] C. Y. Tsai, C. Y. Tsai, F. C. Yu, Y. F. Lan, P. J. Huang, S. Y. Lin, Y. T. Chen, T.I. Tsao, C. T. Hsieh, B. S. Tseng, C. W. Kuo, C. H. Lin, C. C. Kuo, C. H. Chen, H. Y. Hsieh, C. T. Chuang, N. Sugiura, "A novel blue phase liquid crystal display applying wall-electrode and high driving voltage circuit," *SID Int. Symp. Dig. Tech. Pap.* #37.1 (2015).
- [18] D. Xu, J. Yuan, M. Schadt and S. T. Wu, "Blue phase liquid crystals stabilized by linear photo-polymerization," *Appl. Phys. Lett.* **105**, 081114 (2014).
- [19] Y. Hirakata, D. Kubota, A. Yamashita, T. Ishitani, T. Nishi, H. Miyake, H. Miyairi, J. Koyama, S. Yamazaki, T. Cho and M. Sakakura, "A novel field-sequential blue-phase-mode AMLCD," *J. Soc. Info. Disp.* **20**, 38-46 (2012).
- [20] Z. Luo, D. Xu, and S. T. Wu, "Emerging quantum-dots-enhanced LCDs," *J. Disp. Technol.* **10**, 526-539 (2014).